Paper No. 725. (quote when citing this article)
Eleventh World Conference on Earthquake Engineering
ISBN: 0 08 042822 3

NON-LINEAR SITE EFFECTS AT PORT ISLAND VERTICAL ARRAY DURING 1995 HYOGO-KEN NANBU EARTHQUAKE

JORGE AGUIRRE

Jorge Aguirre Gonzalez, graduate student,
Disaster Prevention Research Institute, Kyoto University.
Uji city, Gokasho, DPRI Kyoto University, Kyoto 611, JAPAN.
Tel./Fax. (0774)-33-5866. e-mail jorge@egmdpri01.dpri.kyoto-u.ac.jp.

ABSTRACT

An analysis was made of the propagation of seismic waves in a vertical array using the acceleration waveforms recorded during the 1995 Hyogo-ken Nanbu earthquake. The epicenter was located about 17 km from "Port Island", where the vertical array is situated. Assuming a linear response, we use 7 aftershocks to correct the velocity structure by improving the fitting of the simulations done by 1D linear method (Haskell) to the observed motions from these aftershocks. The adjusted velocity structure was used to simulate the motions during the mainshock in the same way as we did for those of the aftershocks. The simulation satisfactorily explains the vertical component of observed motions, but, not the horizontal components, which are overestimated. Next, the non-linear simulation is performed to explain the behavior of the horizontal components during the mainshock using finite-difference technique for the non-linear simulation. The influence of the non-linear effect in the horizontal components was large and the vertical component behaved almost linearly.

KEYWORDS

Non-linear response; 1995 Hyogo-ken Nanbu earthquake; vertical array data.

INTRODUCTION

The non-linear effect of soil deposits can produce a big change in the response of the ground motions. However the seismologist does not pay enough attention to the non-linear effect because it has not been observed clearly. Bresnev et al. (1995) estimates the onset of non-linearity for the motions larger than 80 Gals, based on laboratory test experiments and using the parameters of a common soft material. On the other hand, non-linear effect at the soil sites has been observed in the field for accelerations larger than 100 Gals (Chin and Aki, 1991, Tamai et al. 1994). The non-linear effect observed on the surface is attributed to the response of the soft soil, while the hard rock underlying the soft soil site is usually considered as free of such effects. Thus, spectral ratios between the rock and soil motions recorded during strong ground motions would be equal to those during weak ground motions if the soil response had linear behavior. Otherwise, the non-linear effect reduces the spectral ratio near the predominant frequency and shift the predominant frequency to lower one. This technique, has been used not only to show a deviation from the linear response (Bresnev et al., 1995) but also to evaluate the linear amplification (Seidl, 1994). However, true motion under the soft soil is generally unknown due to small number of vertical arrays of strong ground motions. This lack of information has forced the researchers to approximately estimate this motions, for instance, from the outcrop ground motions. This assumptions introduce some uncertainties in evaluating the soil response. Fortunately there is a vertical array located in Port Island, providing us very good records during the Hyogo-ken Nanbu earthquake. Here we analyze this data with the purpose of evincing the non-linear effect during the mainshock. Also, we will show the variation of the spectral ratio with the lapse of time after the mainshock occurrence, using long-duration records of 5 minutes subsequent to the mainshock.

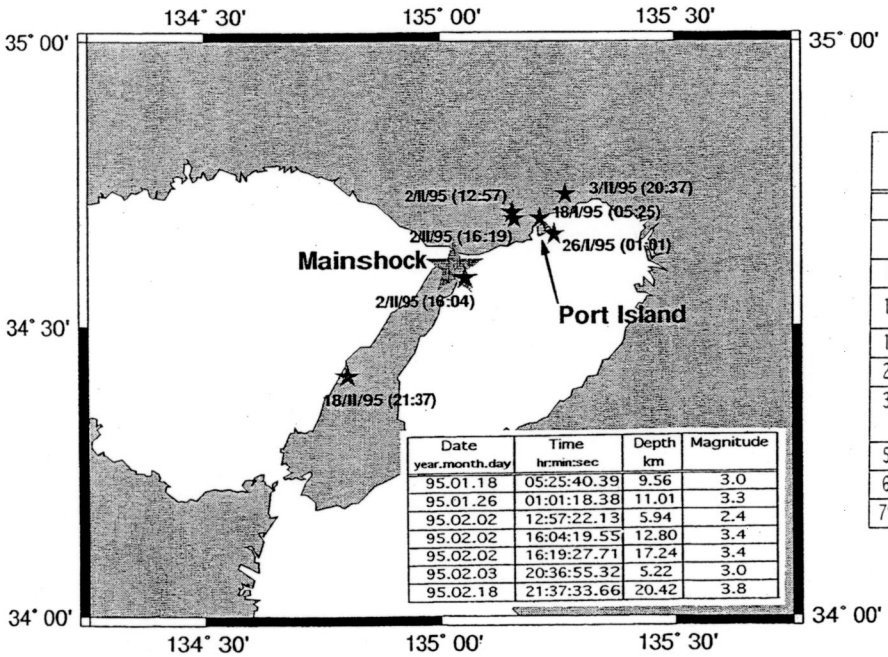

Fig. 1. Location of the 7 aftershocks used in this study. The hypocentral location and magnitudes was determined by DPRI RCEP (1995).

Table 1. Original soil model for the PRT station.

Depth [m]	Soil Type	Location of accelerometers	Vp [km/s]	Vs [km/s]
0 - 2.0	Gravel R	*PR4-0m	0.260	0.170
2.0 - 5.0			0.330	
5.0 - 12.6			0.780	0.210
12.6 - 19.0	Sandy Gravel R	*PR3-16m	1.480	
19.0 - 27.0	Clay		1.180	0.180
27.0 - 33.0	Sand	*PR2-32m	1.330	0.245
33.0 - 50.0	Sandy Gravel and Sand		1.530	0.305
50.0 - 61.0	Sand		1.610	0.350
61.0 - 79.0	Clay			0.303
79.0 -(85.0)	Sandy Gravel	*PR1-83m	2.000	0.320

R Reclaimed land

Vertical array in Port Island

For this study, we use the data recorded at a vertical array located in Port Island. Port Island is a result of reclamation work which was finished in 1980 (Nakakita and Watanabe, 1977) in order to be used as residential, industrial, and port areas. The total area is 436 hectares. A vertical array of accelerometers is located at Port Island (see Fig. 1). It consists of 4 stations located at 83, 32 and 16 m depth in boreholes and at the surface. Each one is equipped with 3-component accelerometers. The sampling frequency of the recorded motions is 100 Hz. The geological stratigraphy and the P and S wave velocity structure provided from boring data are shown in Table 1.

Sets of data

The data used in this study are the records from the mainshock of the Hyogo-ken Nanbu earthquake and their aftershocks. Long time duration records of 360 seconds were obtained at the Port Island station including the mainshock and subsequent aftershocks. These aftershocks will be referred in this paper hereafter as AJAM (aftershocks just after the mainshock). The other aftershocks used here occurred one day and more after the mainshock and we will call them simply "aftershocks". The epicenter locations of 7 aftershocks analyzed are shown in Fig. 1. with supplementary note of date, origin time, depth, and magnitude.

The Hyogo-ken Nanbu earthquake

The Hyogo-ken Nanbu earthquake occurred at 5:46 am (local time) on January 17, 1995 with magnitude MJ 7.2. The hypocenter location reported by Disaster Prevention Research Institute and Research Center for Earthquake Prediction (DPRI RCEP, 1995), is slightly north of Awaji island, as shown in Fig. 1, about 17 km away from the array and 13.3 km depth. Due to the strong ground motions produced by this earthquake, there was observed liquefaction in several places in the Kobe area, in particular in reclaimed lands including Port Island (Takada et al., 1995, Kamon et al., Kokusai Kogyo Co., 1995).

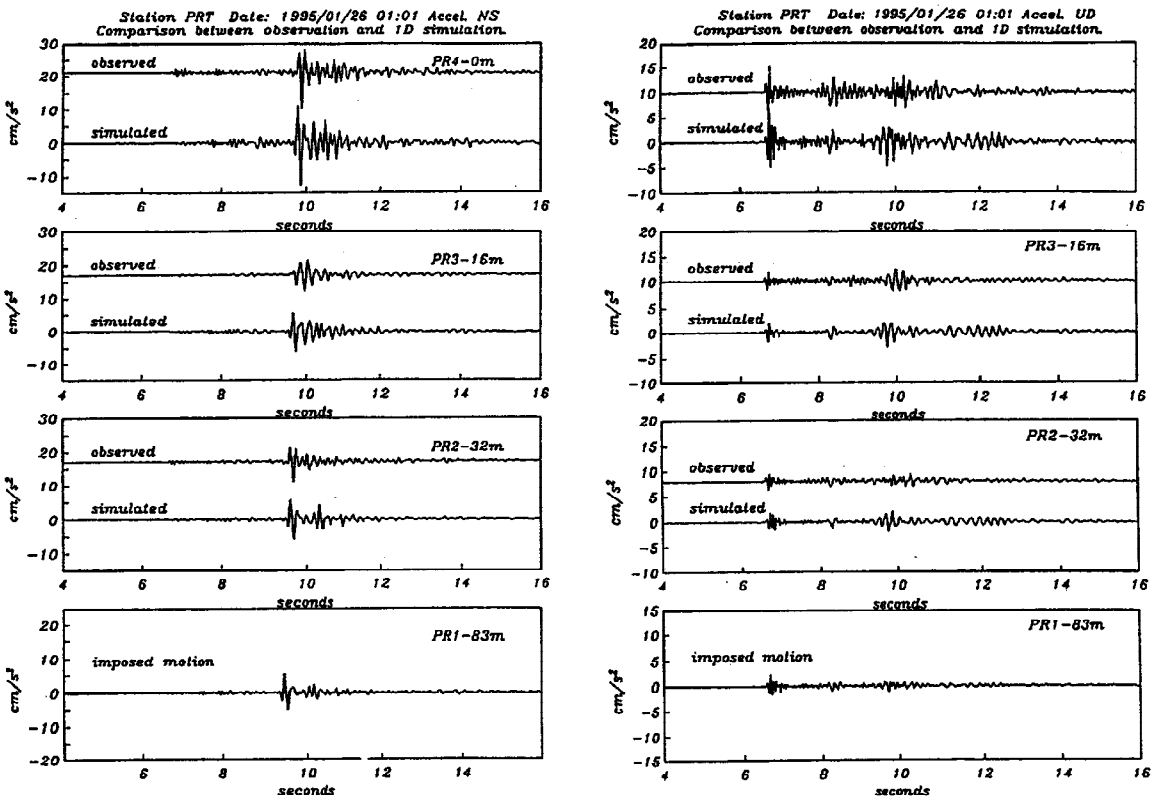

Fig. 2. Linear 1D simulations for the aftershock occurred on January 26, 01:01 hr. at the vertical array, using the velocity structure model in table 1.

ANALYSIS

In order to test the velocity structure model for linear case, we perform the simulation of the ground motion during the aftershocks by using the Thompson-Haskell method. The ground motions are simulated at the stations located at the surface, 16 and 32 meters depth imposing the observed ground motion at 83 meter depth. S waves from a source are almost vertically propagating near surface because the soil deposits beneath the array have very low wave velocities with a striking velocity contrast to the bed rock underlying about 2000 m deep.

Then, the horizontal motions are simulated assuming the vertical incidence of SH waves. On the other hand, the vertical motion are simulated assuming the vertical incidence of P waves, although the vertical motions have large amplitude not in P waves portion but in S waves portion. S waves motions vertically propagating to surface could have no vertical motions. It means that vertical motions are not P waves coming from the source but S-converted P waves beneath the soil deposits.

The simulated ground motions at the 3 surficial stations were compared with the observations. By minimizing the residual values between the simulations and observations, we improve the initial velocity structure after several trials. Our improved velocity structure model is shown in Table 2.

One example of the simulations for the aftershock occurring at 01:01 hr. on January 26 is shown in Fig. 2. We find that the simulated motions agree well with the observed motions both in amplitudes and phases. The discrepancy of the arrival times between the observed and simulated motions around t=10 seconds in the UD component is because only P-wave velocity was used to simulate this component and this phase was propagated with S-wave velocity. But generally speaking, the assumption of the vertical incidence of SH and P waves respectively for the horizontal and vertical motions is reasonable.

Test of linear model during the mainshock

In the previous section we test and demonstrate that our improved velocity structure model can explain the motions at the surface station as well as at the borehole stations for the 7 aftershocks. Now we apply the same improved velocity structure model to verify if the linear behavior can explain the strong mo-

Table 2. Improved soil model for the PRT station.

Thickness [m]	*Density [g/cm^3]	Vp [m/s]	Damping factor	Vs [m/s]	Damping factor
2.0	1.80	300.0	0.17	105.0	0.07
3.0	1.80	330.0	0.17	140.0	0.07
7.6	1.80	780.0	0.17	169.0	0.07
3.4	1.80	1480.0	0.10	176.0	0.07
3.0	1.80	1480.0	0.10	191.0	0.05
8.0	1.50	1180.0	0.10	165.0	0.02
5.0	1.85	1330.0	0.10	342.0	0.02
1.0	1.85	1330.0	0.10	196.0	0.02
17.0	1.85	1530.0	0.10	333.0	0.02
11.0	1.85	1610.0	0.10	466.0	0.02
18.0	1.80	1610.0	0.10	306.0	0.02
6.0	1.90	2000.0	0.10	320.0	0.02

*from Official Written Report of Kobe city, department of Development.

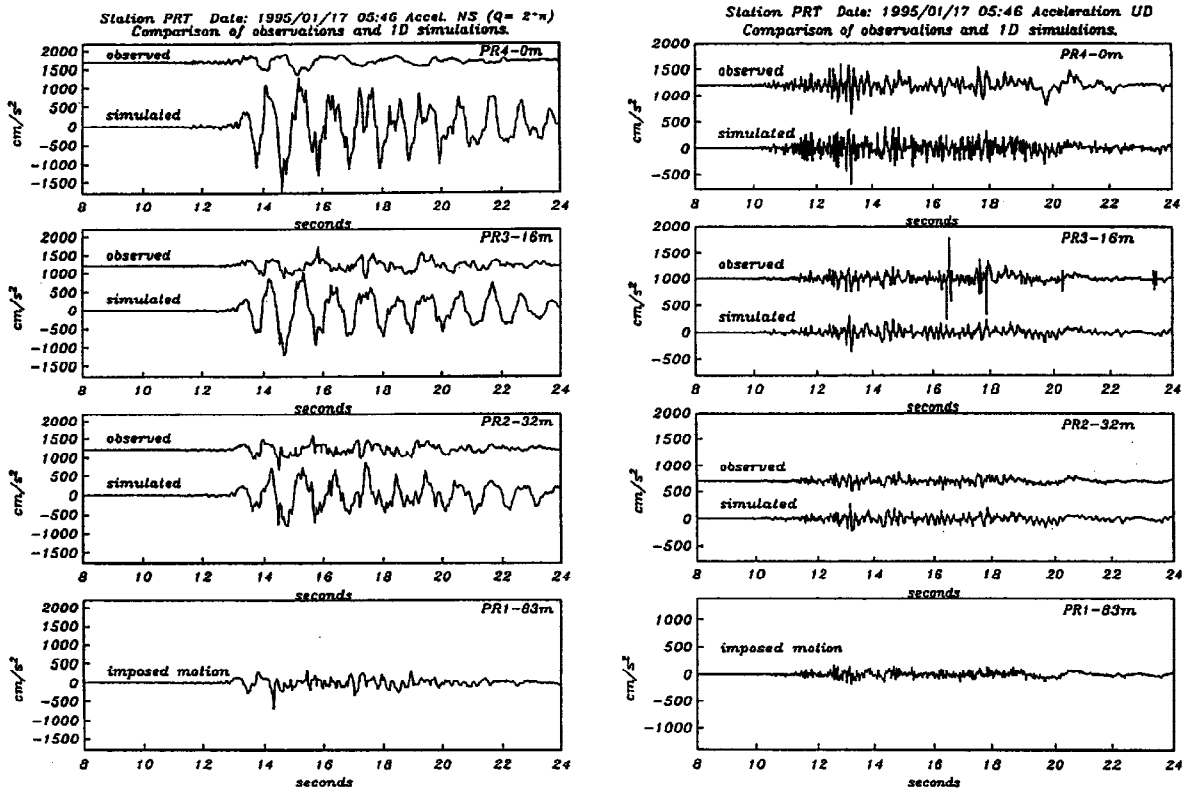

Fig. 3. Linear 1D simulations for the 1995 Hyogo-ken Nanbu earthquake at the PRT vertical array, using the velocity structure model in table 1.

tions at the Port Island array. As we did for the aftershocks we imposed the observed ground motions at 83 meters depth and simulated the ground motions at the surface, 16 and 32 meters depth. The simulated and observed ground motions for this mainshock at the Port Island array are shown in Fig. 3. The linear simulation of the vertical ground motions (UD) shows a reasonable agreement in waveform and amplitude with the observation. Some glitch-like signals seen around 16 s after the recorder starting at the 16 m depth may be related to instrumental noise, from the fact that they were not observed in the records at the other stations in different depths.

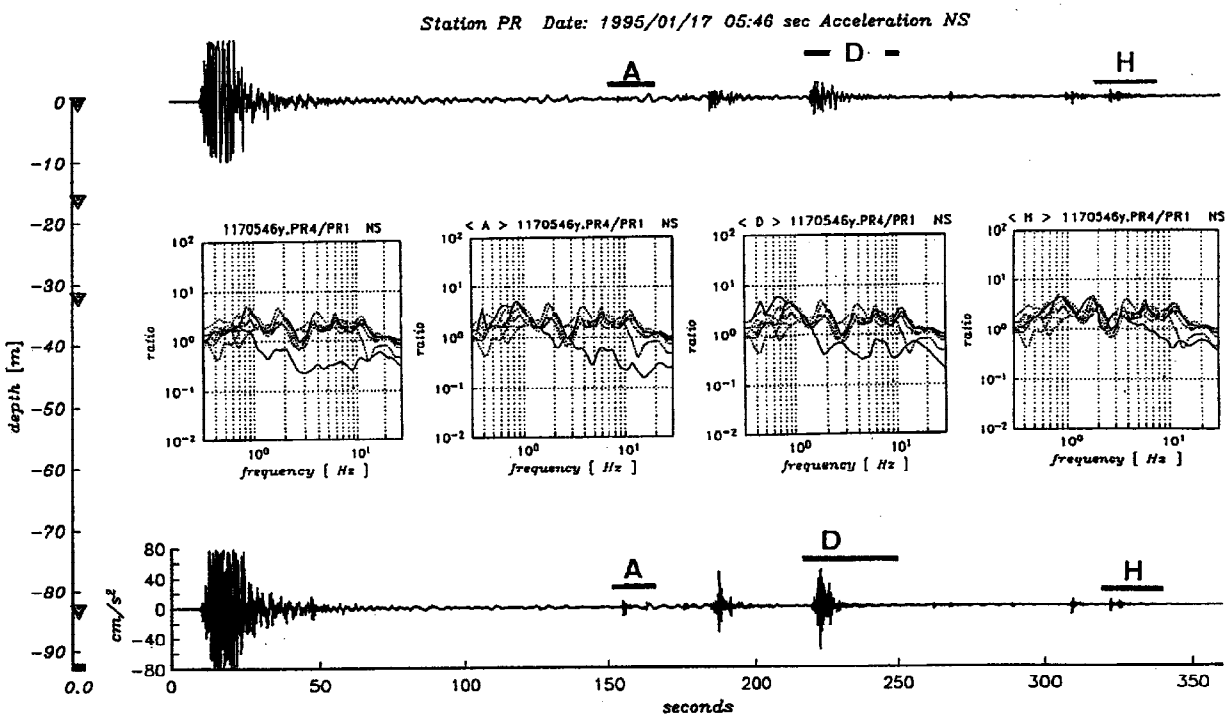

Fig. 4. Variation of the spectral ratios with the lapse of time during the mainshock and AJAM. The Fourier Spectral ratios are computed from the records of station at the surface (top) and at the 83 m depth (bottom). The dashed line shows the ratios for 7 aftershocks of the Fig. 1, and the continuous line the ratios for the mainshock, and for the divisions A, D and H, indicated in the records, for the component NS.

We find that the horizontal motions are remarkably affected by the non-linearity of the soil deposits, and the linear simulation overestimates the peak amplitudes of the ground motions by a factor of more than 4 in the NS component and 3 in the EW component for the surface station. In both horizontal components the overestimation of the simulation decrease with increasing depth. But the amplitudes of the simulated ground motions at 32 meters depth are still larger than those of the observed ground motions. Then, it is clear that the ground motions at the Port Island array during the Hyogo-ken Nanbu earthquake are not explained by a linear soil behavior.

Time variation of spectral response

To examine the spectral characteristics of the soil in Port Island we calculate the spectral ratios between the surface and the 83 m depth stations for our 3 sets of data. The ratios from the 7 aftershocks after one day following the mainshock are taken as a reference for the linear behavior, being plotted by dotted lines in Figs. 4 and 5. The long duration records of 360 seconds during and after the mainshock at the surface and 83 m depth are shown at the top and bottom of the Figs. 4 and 5. They include the mainshock and subsequent aftershocks (AJAM). To analyze the behavior of these AJAM, we divided arbitrarily the record into 9 divisions, mainshock and division A to H (see the top and bottom of Figs. 4 to 6). The ratios of the surface to 83 m depth were obtained for each division in the same way as we did for the aftershocks. In the middle of the Figs. 4 to 6 we show the ratios of the mainshock to three divisions A, D and H. For instance, the division A is a time length of 18 seconds, from 150 to 168 seconds after the recording started. We compare those ratios with the reference ratios given from the 7 aftershocks by dotted lines. The reference ratios are considered to show linear soil responses. We find the following features of the responses of the horizontal motions with lapse time after the mainshock in Fig. 4. Low frequency responses less than 1 Hz are almost the same as the reference ratios, indicating linear soil behavior for low frequency motions. Higher than 1 Hz frequency responses show remarkable differences during the mainshock from the linear response, being gradually recovered with lapse of time from A to H. The deamplification after the mainshock seems to occur independent of the levels of acceleration. Then, the phenomenon that controls such amplitude reduction is different from non-linearity during the mainshock. The largest deamplification

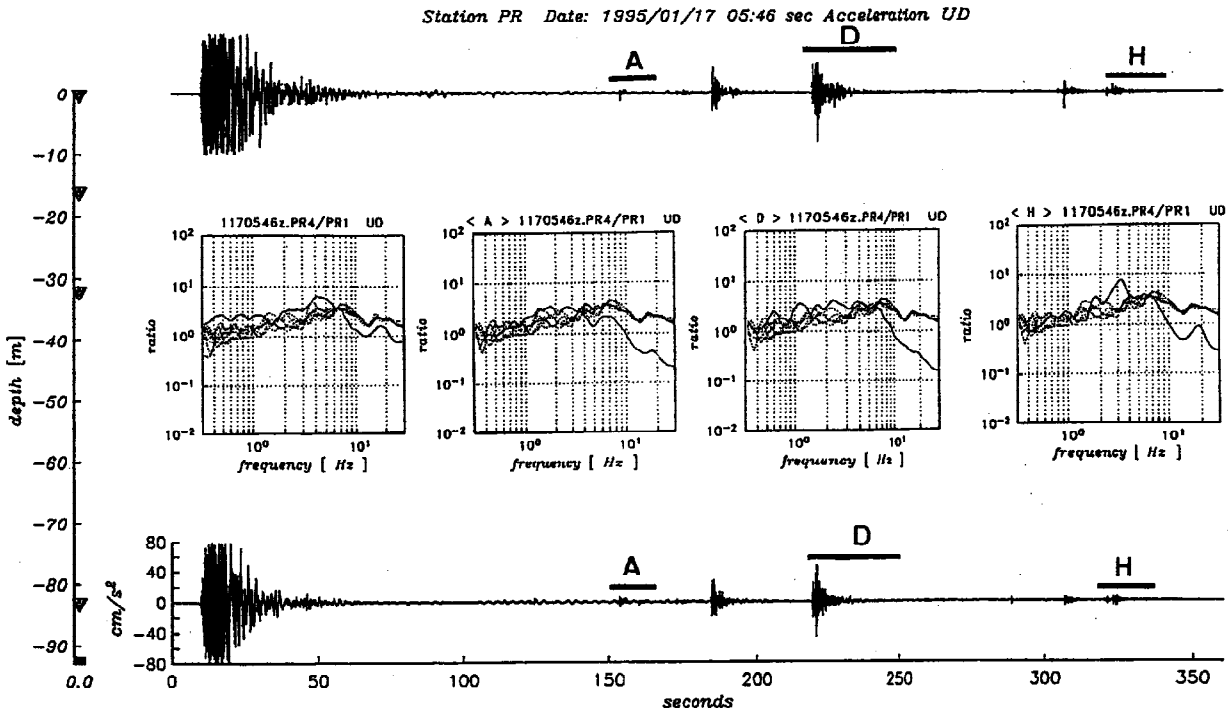

Fig. 5. Same as Fig. 4, but for UD component.

is seen in Division A around 15 Hz. From the tendency of the time variation of the response we inferred that the linear soil behavior may be recovered several minutes soon after the last division H. The response of the vertical motion during the mainshock, in Fig 5, is almost similar to the reference ones, indicating less influence of non-linearity. However, the response in the Division A show clear deamplification at high frequencies more than 5 Hz. This means that the soil behavior for the both the horizontal and vertical motions completely changed a few minutes after the mainshock, probably because of water coming up.

Non-linear simulation

We simulate the non-linear response of the soil deposits during the mainshock using an algorithm that calculate the rigorous non-linear response. The method uses a finite-difference technique and step by step time integration. The non-linear relation of the stress-strain is prescribed by the backbone curve proposed by Hardin and Drnevich. The shape and dimension of the curve is fixed by the failure strength and the damping factor. Then we can model the curve according to the characteristics of the material by changing these two parameters. The details of the method are described in Perez-Rocha and Sanchez-Sesma (1992) and Joyner and Chen (1975). In this simulation in particular, we imposed the observed motion at 83 m depth and obtained the ground motions at the surfitial stations of a stratified media with non-linear response. We perform the non-linear simulation trying to fit the simulated ground motions to the observations without any a priori information about the dynamic characteristics of the soil. The linear parameters, such as density, S, and P wave velocities were taken from the previously improved velocity structure in Table 2. Using trial and error, we tried to obtain such non-linear parameters that can explain the amplitude levels and waveforms of the observed ground motions at the stations located at the surface, 16 and 32 meters depth. After several trails we obtained the parameters listed in Table 3 that can produce the non-linear simulation matching the observations well as showing in Fig. 6. The agreement in amplitude level between the simulation and observation is good at all the stations. The simulated waveforms for the 16 and 32 m depth have a good agreement in main phases with the observed ones. The simulated ones for the surface station agrees well until 16 s, however after that shows serious differences from the observed motions in phases and amplitudes. We attribute such differences to the liquefaction that could be responsible for almost disappearance of the propagation of S waves mainly contributing to the horizontal motions. Some

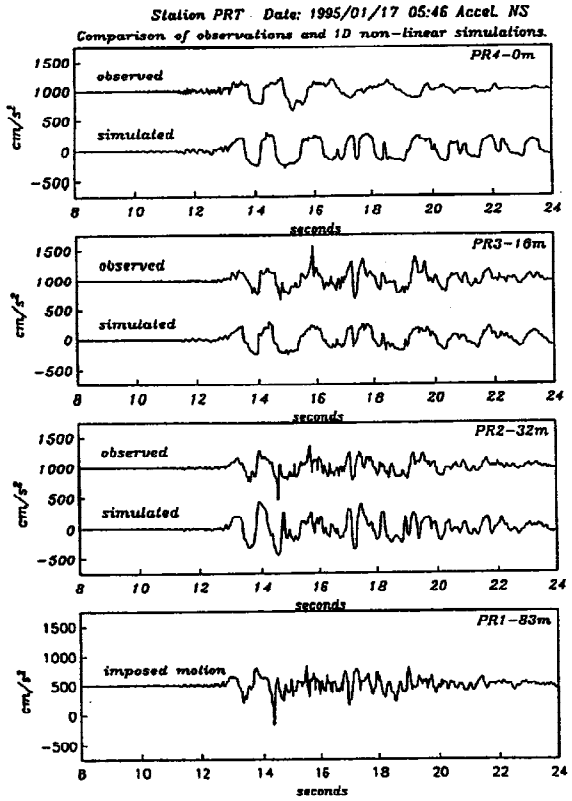

Fig. 6. Non-linear simulations for the 1995 Hyogo-ken Nanbu earthquake at the PRT vertical array, using the parameters of the Table 3.

Table 3. Parameters of the structural model used for the non-linear simulation.

Thickness [m]	Density [g/cm^3]	Vs [m/s]	Damping factor	Failure Strength [dyn/cm^2]
2.0	1.80	170.0	0.08	6.0×10^4
3.0	1.80	170.0	0.08	6.0×10^4
7.6	1.80	210.0	0.08	8.0×10^5
6.4	1.80	210.0	0.08	8.0×10^5
8.0	1.50	180.0	0.08	9.0×10^5
6.0	1.85	245.0	0.08	9.0×10^5
17.0	1.85	305.0	0.05	2.0×10^6
11.0	1.85	350.0	0.05	2.0×10^7
18.0	1.80	303.0	0.05	1.0×10^8
6.0	1.90	320.0	0.05	1.0×10^8

sharp peaks appearing in the observed motions at 14.5 and 16 s at 32 and 16 m depth respectively for the case of NS component, are not well reproduced by our non-linear simulation. Those may be are related with the cyclic mobility phenomenon not considered here. Another explanation is that the peaks in the simulation are specially affected by an excessive damping.

DISCUSSION AND CONCLUSIONS

We try to simulate the non-linear response, facing the fact that we did not have any information about the dynamic characteristics of the stratified media, although we have the observed ground motion. Then by trial and error we found the parameters for the non-linear simulation that can explain the observed ground motions. The above non-linear simulation can explain the characteristics of the observed horizontal waveforms through the main motions during the mainshock for the horizontal components at 32 and 16 m depth but those at the surface for only the first several seconds after the mainshock arriving, until about 16 s after the recorder starting in Fig. 6. After that, the observed motions at the surface show some differences from the simulated ones. We observed two stages in time history variation, one starts around 13 s and the other occurs around 16 s in the recording of Fig. 6. The second stage is characterized by a substantial reduction of amplitude, where our simulation fails to explain the observed record. We interpreted the first change as the starting of the non-linear stage and the second one, as the starting of the liquefaction stage. Our non-linear simulation can reduce the amplitudes and change the frequencies of the waveform in accordance with the non-linear stage in the observations. However, the non-linear stage is mixed with the initial liquefaction or cyclic mobility. Ishihara (1985) showed how the cyclic mobility produced sharp peaks like the observed in the 16 m depth records in the Fig. 6, at 15.9 for NS component, causing by the increasing of the pore water pressure. When the liquefaction stage occurs, no effective stress is acting on the sand and individual particles released from any confinement exist as if they were floating in water (Ishihara, 1985). In this stage, the S waves can not be transmitted efficiently and therefore a big reduction of the amplitudes is expected in the horizontal components if we accept the assumption of vertical propagation of the wave field. After the onset of liquefaction the amplitude reduction at the surface is not controlled by the level of stress. This situation remains until the soil recover the linear characteristics about 10 minutes later.

The soil is healing gradually with elapsed time after liquefaction. Phenomena like this might happen in other sites in Kobe area.

We have been showed that the responses of the soil deposits in Port Island behave linearly during the 7 aftershocks after one day following the mainshock. The velocity structure was well characterized by the parameters shown in Table 2. The validity of the structure model is confirmed from comparing the observed aftershock motions with the simulated ones by the Thompson-Haskell method. In the case of the mainshock the linear simulation of the ground motions at the surface produces an overestimation by a factor of about 4 to the observed peak amplitudes in the horizontal components. However, the peak amplitude of the simulated vertical motions is quite similar to the observed one. The analysis of the spectral ratios between the surface and 83 m depth during the mainshock and the AJAM shows the variation of the non-linearity with the lapse of time suggesting that the soil characteristics changed after the mainshock. Also, it indicated the gradual recovering of the linear response with the lapse of time. Based on that, it is expected to recover the linear response only about 10 minutes after the mainshock occurrence. The difference in the spectral ratio for the vertical component during the mainshock from the linear response is small, but it increases during the first AJAM and later follow the same tendency of recovering the linear response as those for the horizontal components. Extension of this results may be used to interpret the unbalanced amplification of the vertical component in comparison with the horizontal ones, observed in other stations with similar conditions during this earthquake.

REFERENCES

Aguirre, J., Irikura, K. and Kudo, K., Estimation of Strong Ground Motions on Hard Rock and Soft Sediment Sites in the Ashigara Valley Using the Empirical Green's Function Method, *Bull. Disas. Prev. Res. Inst., Kyoto Univ.*, **44**, Part 1, No. 379, pp. 45-68, 1994.

Bresnev, I. A., Wen, K.-L., and Yeh, Y. T., Nonlinear Soil Amplification: Its Corroboration in Taiwan, *Bull. Seismol. Soc. Am.*, **85**, pp 496-515, 1995.

Chin, B.-H. and Aki, K., Simultaneous study of the source, path, and site effects on strong ground motion during the 1989 Loma Prieta Earthquake: a preliminar result on pervasive non-linear site effects., *Bull. Seismol. Soc. Am.*, **81**, pp 1859-1884, 1991.

Development Bureau, Kobe city, Report of the soil investigation and installment of strong motion accelerograph, 1991.(in Japanese)

D.P.R.I. R.C.E.P., Preliminar report on the January 17, Hyogoken-nambu earthquake. *The Coordinating Committee for earthquake prediction,* No. 113, pp. 1-22, 1995. (in Japanese)

Ishihara, K., Stability of natural deposits during earthquakes. *Proc. of 11th Int. Conf. on Soil Mechanics and Foundation Engenering*, **1**, pp 327-376.

Joyner, W. B., and Chen, A. T. F., Calculation of Nonlinear Ground Response in Earthquakes, *Bull. Seismol. Soc. Am.*, **65**, pp 1315-1336, 1975.

Kamon, M., Mimura, M., and Katsumi, Takeshi, Geotechnical Disasters Caused by the 1995 Hyogoken-nambu Earthquake, *Journal of Natural Disaster Science*, **16**, pp. 71-77, 1995.

Katayama,T., Yamazaki, F., Nagata, S., Lu, L. and Turker, T., A Strong Motion Database For the Chiba Seismometer Array and its Engineering Analysis, *Earthquake Engineering and Structural Dynamics*, **19** pp. 1089-1106, 1990.

Kokusai Kyogo CO. LTD, Disaster Map of Great Hanshin Earthquake, No. I, No. II, and No. III, 1995.

Nakakita, Y., and Watanabe, Y., 1977, Soil Stabilization by Preloading in Kobe Port Island *Proc. 9th Int. Conf. on Soil Mechs. and Fund. Eng.*, Vol. case hist., pp. 611-622.

Ordaz, M. and Faccioli, E., Site Response Analysis in The Valley of Mexico: Selection of Input Motion and Extent of Non-Linear Soil Behavior, *Earthquake Engineering and Structural Dynamics*, **23** pp. 895-908, 1994.

Perez-Rocha, L. E. and Sanchez-Sesma, F. J., Hybrid non-linear response of soft soils, *Proc. 10th World Conf. on Earthq. Eng.*, **2**, pp. 973-979, 1992.

Yu, G., Anderson, J. A., and Siddharthan, R., On The Characteristics of Nonlinear Soil Response, *Bull. Seismol. Soc. Am.*, **83**, No. 1, pp 218-244, 1993.

Steidl, J. H. and M.EERI, Variation of Site Response at the UCSB Dense Array of Portable Accelerometers, *Earthquake Spectra*, **9**, pp. 289-302, 1993.

Takada, S, Hassani, N., and ABDEL-AZIZ, M., Quick Report of the Damage Caused by the 1995 Hyogo-ken Nambu Earthquake, *Journal of Natural Disaster Science*, **16**, pp. 59-70, 1995.

Tamai, M., Horike, M., Takeuchi, Y., Suzuki, H., and Uetake, T., Verification of non-linearity of surficial layer using vertical-array strong-motion data, *Proc. 9th Japan Earthq. Eng. Sym.*, **1**, pp. 229-234, 1994.